

## **Optics, Acoustics and Stress in Situ (OASIS)**

John H. Trowbridge<sup>1</sup> and Peter Traykovski<sup>2</sup>  
Woods Hole Oceanographic Institution  
Woods Hole, MA 02543  
phone: 508-289-2296<sup>1</sup> or 2638<sup>2</sup>, fax: 508-457-2194  
e-mail: [jtrowbridge@whoi.edu](mailto:jtrowbridge@whoi.edu), [ptraikovski@whoi.edu](mailto:ptraikovski@whoi.edu)

Award numbers: N000140410221 and N00014-10-10768  
<http://www.whoi.edu/hpb/viewPage.do?id=81116&cl=1>

### **LONG-TERM GOALS**

To quantify and understand the effects of aggregation dynamics on the distribution of particles in the bottom boundary layer, and to understand how the properties of particles (composition, shape, and internal structure) affect their optical and acoustical properties.

### **OBJECTIVES**

- Obtain direct measurements of the turbulent Reynolds stress within the wave boundary layer (WBL)
- Obtain concurrent velocity, turbulence and seafloor microtopography (bedforms) measurements to constrain the fluid dynamical environment within which the particle size distribution evolves.
- Improve state-of-the-technology for measuring boundary layer velocity and turbulence profiles (Pulse Coherent Doppler Profiler) and seafloor bedform measurements (Rotary Sidescan and Pencil-beam sonars)

### **APPROACH**

Our project is focused on obtaining direct measurements of the turbulent Reynolds stress within the wave boundary layer (WBL), which has not been possible in previous field studies. The measurements of stress are combined with detailed topographic maps of the bedforms to understand the relations between the bedforms and the turbulent flow over the bedforms. This is motivated by the order-of-magnitude difference between relatively small stresses that have been measured above the WBL and the much larger stresses that have been inferred within the WBL. The discrepancy between measured and modeled stresses above the WBL has been attributed to processes within the WBL. Hill et al., (2001) inferred the large stresses within the WBL play a dominant role in controlling particle size and thus strongly influence particle settling velocities, concentrations, and optical properties.

The measurements capitalized on multi-frequency pulse-coherent Doppler profiling (PCDP) sonars developed recently at WHOI by Peter Traykovski and Fred Jaffre (2011) based on a high frequency sonar board designed by Gene Terray and Tom Austin and Peter Traykovski. The multi-frequency

methodology (Hay and Zedel, 2008) removes the ambiguity associated with conventional pulse-coherent sonar measurements. The combination of range-gated vertical (transmit-receive) and slanted (receive-only) acoustical beams produces vertically resolved measurements of the horizontal and vertical velocity throughout the wave boundary layer and the lower part of the overlying current boundary layer (Figure 1). The effective sample volume is the product of the beam patterns along the acoustical transmission and reception paths, and is small because of the narrow vertical beam. The new sensors produce high-precision velocity measurements along with order-one-meter range, sub-centimeter spatial resolution, and a sample rate of approximately 18 Hz. With proper configuration, these sensor characteristics are sufficient for measurements of both the oscillatory velocity and the turbulent velocity fluctuations in the WBL at field scales.

## **WORK COMPLETED**

The instrumentation was deployed in 11 m water depth at the Martha's Vineyard Coastal Observatory (MVCO) in September and October of 2011 for a period of one month (Figure 2). Data processing and analysis was conducted and the results were presented at the 2012 American Geophysical Union Ocean Sciences Meeting in poster entitled "Observations of Wave Boundary Layer Turbulence and Sediment Suspension" The 2011 ONR annual report describes the details of the equipment development and preparation for this work (<http://www.onr.navy.mil/reports/FY11/lotrayk2.pdf>).

## **RESULTS**

The rotary sonar imagery shows orbital scale bedforms in the coarse sand ( $D_{50} = 650 \mu\text{m}$ ) present in the rippled scour depressions at MVCO. These bedforms have wavelengths that vary from 0.40 to 1.2 m and scales with the orbital diameter of the waves. Figure 3 shows an example with 0.7 m wavelength.

Horizontal and vertical velocity profiles from the PCDP show energetic wave flows and bursts of turbulence shed from the ripple crests (Figure 4). Inertial dissipation method fits to spectra from both time series analysis and direct spatial analysis reveal a relatively low friction factor ( $f_e = 0.01$ ) and consistent with grain roughness in the well-known Swart's (1976) friction factor (Figure 5).

A two dimensional analysis of the turbulent flow over the ripples estimated by using the ripple migration past the PCDP as a proxy for position along the ripple crest allows analysis of the strength of the eddies shed from the ripple crests (Figure 6). These eddies produce stresses that are highly out of phase with free stream velocity and are thus high dissipative. An analysis of the dissipation due to the total ripple roughness, including the eddies produces a friction factor of ( $f_e = 0.1$ ) consistent with laboratory results over orbital scale ripples. This represents one of the first field measurements of wave boundary layer turbulent flow over orbital scale ripples.

## **IMPACT/APPLICATIONS**

Operational seagoing systems often depend on optical and acoustical properties of suspended particles in the water column. Understanding the processes that regulate the particle characteristics and understanding the optical and acoustical signatures of suspended particles are essential in order to predict the performance of these operational systems. The development of instrumentation that can resolve wave boundary layer turbulence has potential to make significant improvements to our understanding of boundary layer and sediment processes.

## RELATED PROJECTS

Much of the development work and equipment purchases described in this work was funded by a DURIP proposal entitled “Instrumentation for Measuring Nearshore Morphologic Change and Hydrodynamic Forcing” (00014-10-10768) and instrumentation will also be used in the “Dynamics of sandwaves under combined wave-current forcing and mine burial processes” (N00014-11-10291) and “Multi-Scale (cm to km) Hydrodynamic and Morphologic Interactions in Tidal Inlets” (N00014-10-10376)

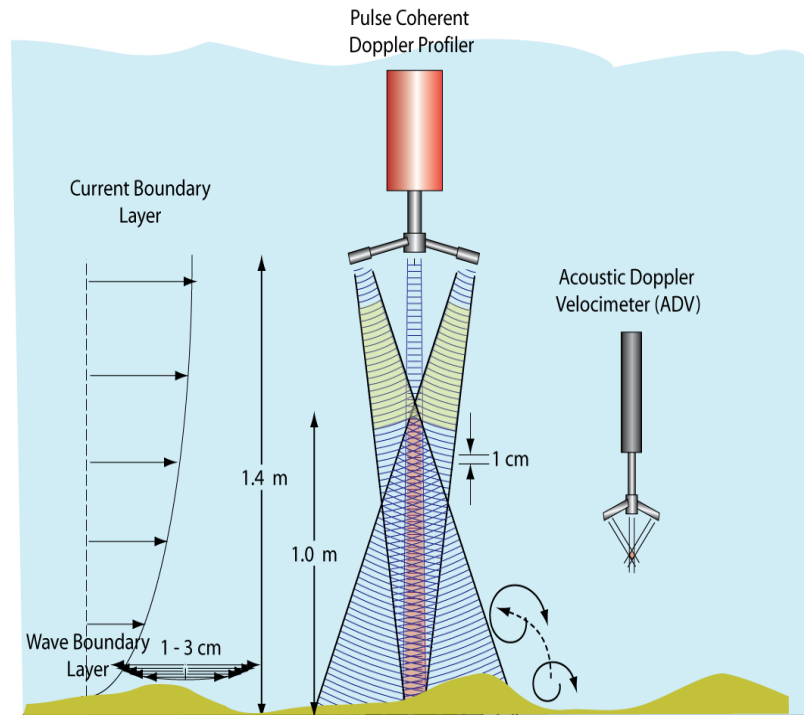


**Figure 1. Schematic diagram of the pulse-coherent Doppler profiler developed at WHOI. The red shaded area represents the region of 1 cm resolution profiles of  $u$ ,  $v$  and  $w$  at turbulence resolving rates (18 Hz). An additional pair of angled transducers is located in the plane perpendicular to the pair shown.**

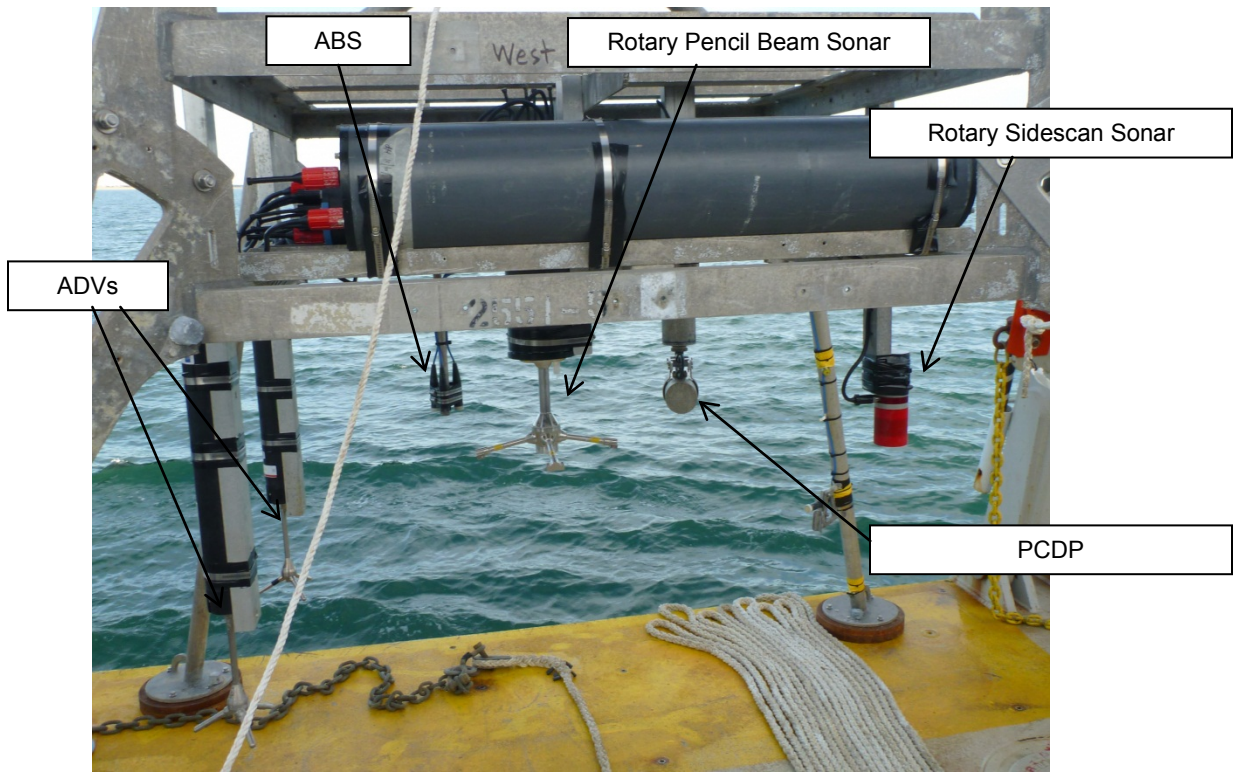


*Figure 2. Photograph of instrumentation just before deployment at MVCO in September 2011, showing Pulse Coherent Doppler Profiler (PCDP), Imagenex rotary sidescan sonar, Imagenex 2-axis rotary pencil beam sonar, Aquatec ABS and Nortek Vector ADVs.*

Rotary Sonar Date:17-Sep-2011 23:17:20

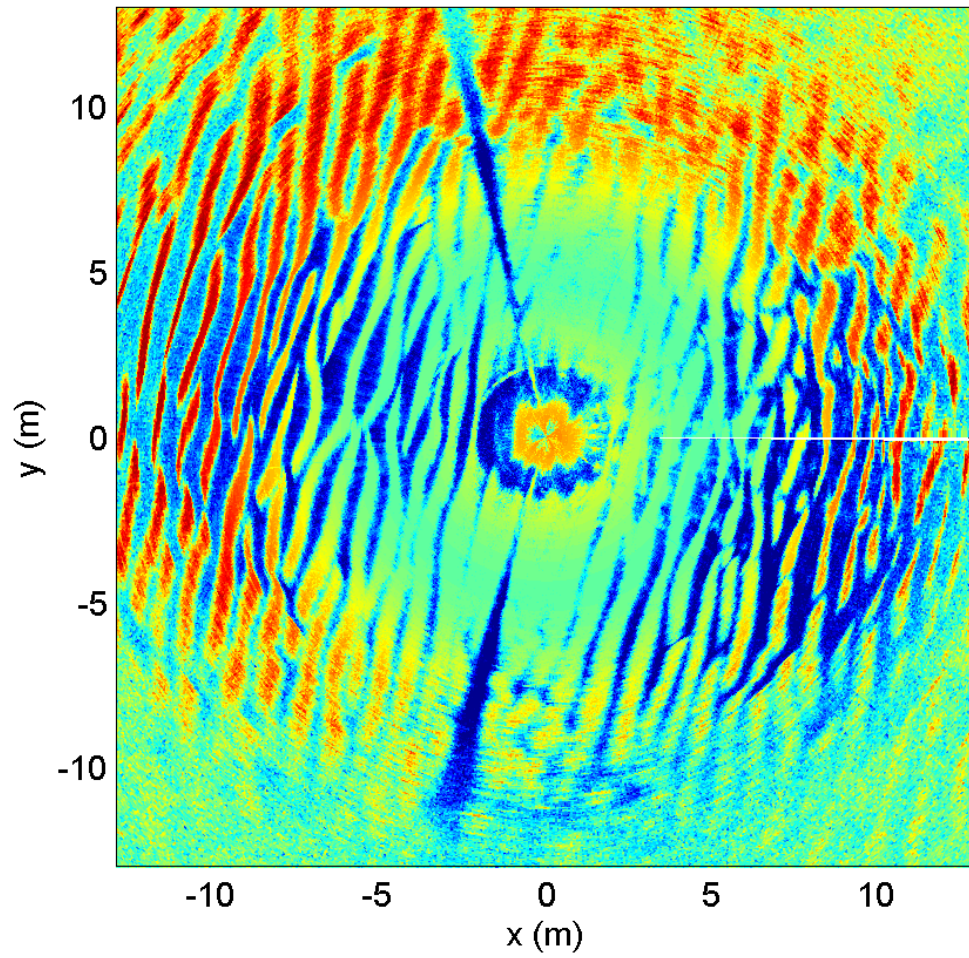


*Figure 3. Rotary Sidescan Image showing 70 cm wavelength orbital scale ( $l \sim 0.75 (2A)$ ) ripples, where  $2A$  is the orbital diameter*

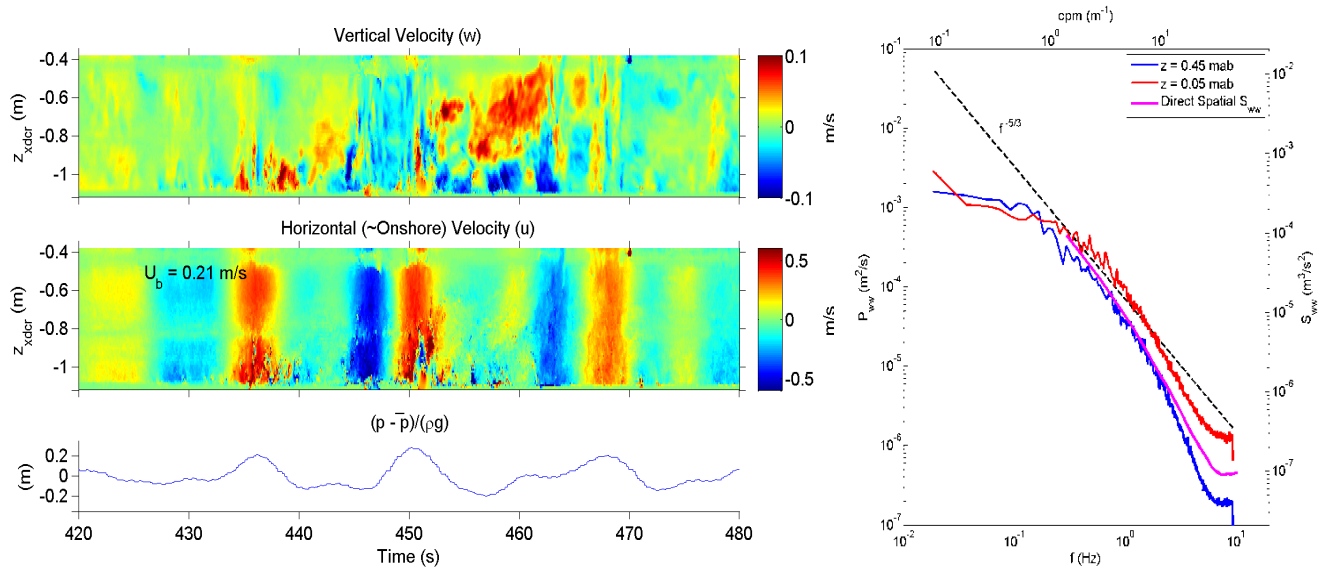


**Figure 4.** *left, top to bottom: vertical velocity profiles, horizontal velocity profiles and pressure right: vertical velocity spectra at (blue) 0.45 m, (red) 0.05 m above the bed and (magenta) spectra based on direct wavenumber spatial spectra.*

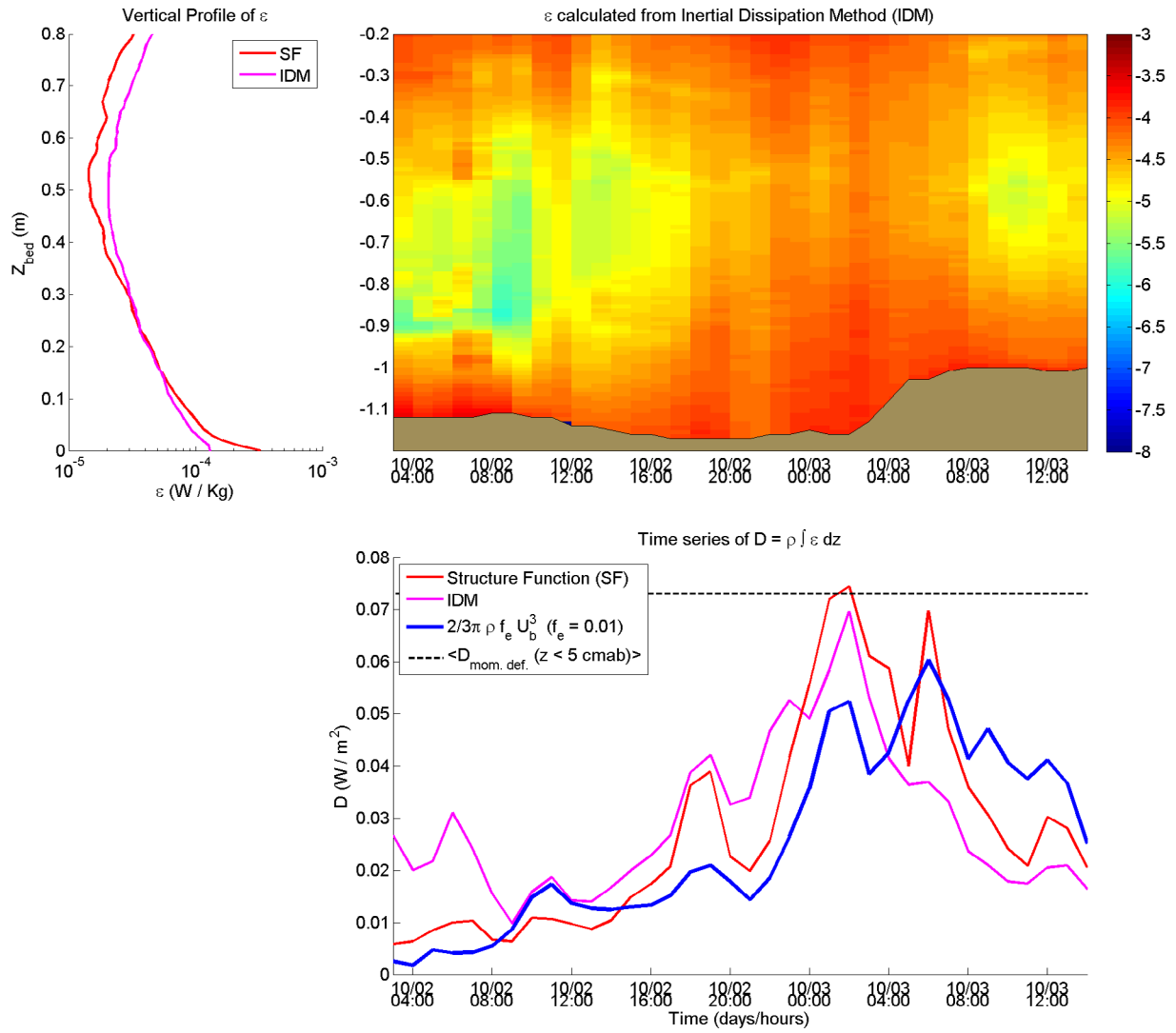


**Figure 5. left: time averaged profiles of dissipation estimated using the inertial dissipation method. right: time series of dissipation profiles. Bottom: time series of depth integrated Dissipation associated with measured turbulent fluctuations is low ( $f_e = 0.01$ ) and consistent with Grain Roughness in Swart's Friction Factor**

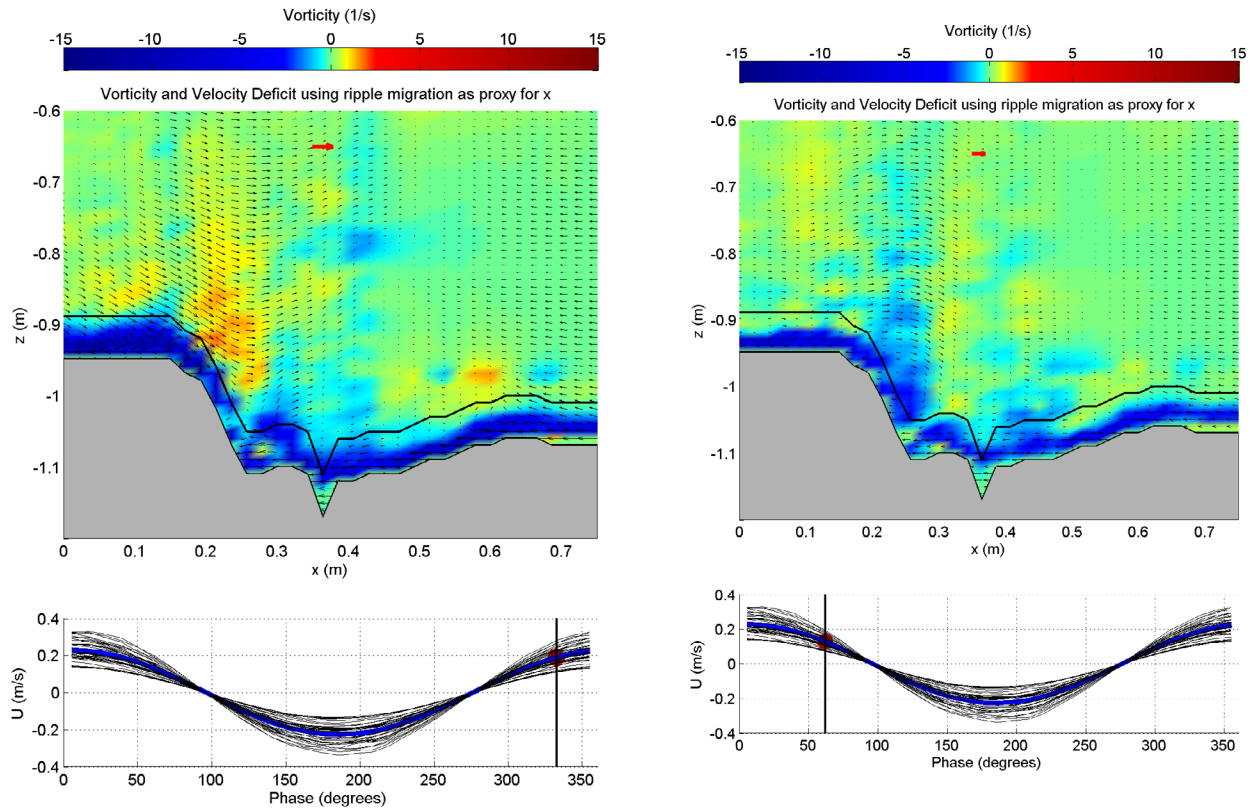


**Figure 6. Left panel: phase averaged flow field and vorticity at a phase of  $330^\circ$  past (or  $30^\circ$  before) maximum onshore velocity. Positive vorticity is visible in the lee of ripple. This vorticity was advected from the separation in the period between  $180$  and  $270^\circ$ . Right panel: phase averaged flow field and vorticity at a phase of  $60^\circ$  past maximum onshore velocity showing negative vorticity consistent with the separation of flow in the lee of the ripple.**

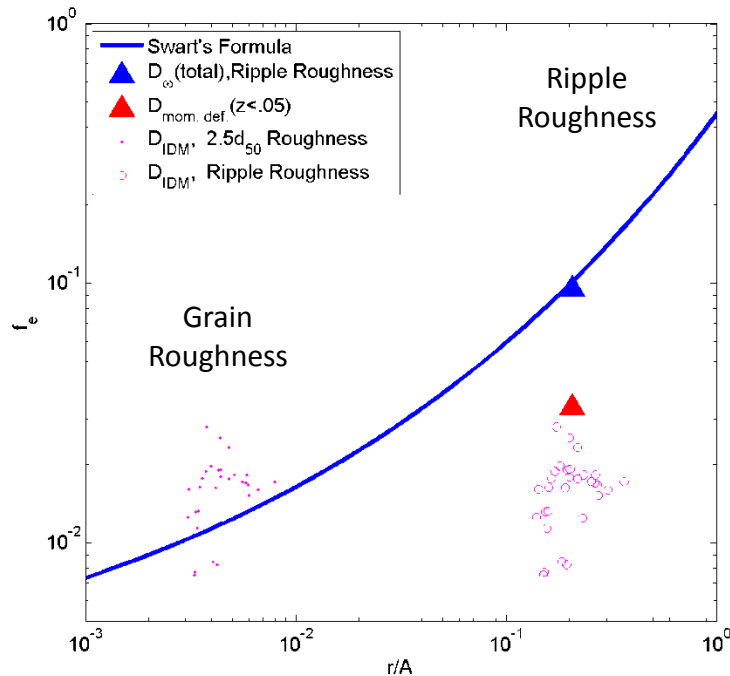


**Figure 7. Dissipation associated with measured turbulent fluctuations is low ( $f_e = 0.01$ ) and consistent with grain roughness in Swart's Friction Factor (magenta dots). When this dissipation associated with measured turbulent fluctuations is placed on the friction factor graph at a roughness associated with ripple height, the data falls well below Swart's formulation (magenta circles). Using a momentum deficit approach in the near bed region produces a slightly higher friction factor (red triangle,  $f_e = 0.03$ ), but in order to produce a friction factor consistent with Swart's formulation the dissipation from the large eddies shed from the ripple crests must be included (blue triangle,  $f_e = 0.1$ ).**

## REFERENCES

- Hay, A. E., L. Zedel, R. Craig and W. Paul (2008), Multi-Frequency, Pulse-to-pulse Coherent Doppler Sonar Profiler, *Proceedings of the IEEE/OES/CMTC Ninth Working Conference on Current Measurement Technology*, Charleston, SC, March 2008
- Hill, P. S., G. Voulgaris, and J. H. Trowbridge (2001), Controls on floc size in a continental shelf bottom boundary layer, *J. Geophys. Res.*, 106(C5), 9543-9549.
- Swart, D.H. 1976. Predictive equations regarding coastal transports, *Proceedings of 15th Conference on Coastal Engineering*, 2:1113-1132.

## PUBLICATIONS

- Traykovski and Jaffre, Development and Field Measurements with Multi-Frequency, Pulse-Coherent Doppler Systems, *The Journal of Ocean Technology*, Vol. 6, No. 2, 2011